Bu Cy

AFWAL-TR-86-4029

ADA177995

AN ELECTRON MICROSCOPIC STUDY OF THE MORPHOLOGY OF CURED EPOXY RESIN

W.W. Adams, V.B. Gupta, and L.T. Drzal
Polymer Branch
Nonmetallic Materials Division

R. Omlor
Systems Research Laboratories
Dayton, OH 45440

December 1986

Interim Report for Period July 1982 - June 1984

MATERIALS LABORATORY
AIR FORCE WRIGHT AERONAUTICAL LABORATORIES
AIR FORCE SYSTEMS COMMAND
WRIGHT-PATTERSON AIR FORCE BASE, OHIO 45433-6533

When Government drawings, specifications, or other data are used for any purpose other than in connection with a definitely related Government procurement operation, the United States Government thereby incurs no responsibility nor any obligation whatsoever; and the fact that the Government may have formulated, furnished, or in any way supplied the said drawings, specifications, or other data, is not to be regarded by implication or otherwise as in any manner licensing the holder or any other person or corporation, or conveying any rights or permission to manufacture use, or sell any patented invention that may in any way be related thereto.

This report has been reviewed by the Office of Public Affairs (ASD/PA) and is releasable to the National Technical Information Service (NTIS). At NTIS, it will be available to the general public, including foreign nationals.

This technical report has been reviewed and is approved for publication.

THADDEUS E. HELMINIAK
Project Scientist

RICHARD L. VAN DEUSEN, Chief
Polymer Branch

FOR THE COMMANDER

GAIL E. EICHELMAN, Assistant Director
Nonmetallic Materials Division

"If your address has changed, if you wish to be removed from our mailing list, or if the addressee is no longer employed by your organization please notify AFWAL/MLBP, Wright-Patterson AFB OH 45433-6533 to help us maintain a current mailing list."

Copies of this report should not be returned unless return is required by security considerations, contractual obligations, or notice on a specific document.

REPORT DOCUMENTATION PAGE

1a. REPORT SECURITY CLASSIFICATION Unclassified	1b. RESTRICTIVE MARKINGS
2a. SECURITY CLASSIFICATION AUTHORITY	3. DISTRIBUTION/AVAILABILITY OF REPORT Approved for Public Resease; Distribution Unlimited.
2b. DECLASSIFICATION/DOWNGRADING SCHEDULE	
4. PERFORMING ORGANIZATION REPORT NUMBER(S) AFWAL-TR-86-4029	5. MONITORING ORGANIZATION REPORT NUMBER(S)
6a. NAME OF PERFORMING ORGANIZATION Materials Laboratory 6b. OFFICE SYMBOL (If applicable) AFWAL/MLBP	7a. NAME OF MONITORING ORGANIZATION
6c. ADDRESS (City, State and ZIP Code) Wright-Patterson AFB OH 45433-6533	7b. ADDRESS (City, State and ZIP Code)
8a. NAME OF FUNDING/SPONSORING ORGANIZATION 8b. OFFICE SYMBOL (If applicable)	9. PROCUREMENT INSTRUMENT IDENTIFICATION NUMBER
8c. ADDRESS (City, State and ZIP Code)	10. SOURCE OF FUNDING NOS. PROGRAM ELEMENT NO. 61102F; PROJECT NO. 2303; TASK NO. Q3; WORK UNIT NO. 07
11. TITLE (Include Security Classification) An Electron Microscopic Study of the Morphology of Cured Epoxy Resin	
12. PERSONAL AUTHOR(S) V. B. Gupta, L. T. Drzal, W. W. Adams and R. Omlor	
13a. TYPE OF REPORT Interim 13b. TIME COVERED FROM Jul 82 TO Jun 84	14. DATE OF REPORT (Yr., Mo., Day) 1986 December 15. PAGE COUNT 44
16. SUPPLEMENTARY NOTATION	

17. COSATI CODES			18. SUBJECT TERMS (Continue on reverse if necessary and identify by block number)		
FIELD	GROUP	SUB. GR.			
11	04		Epoxy	Fracture Surfaces	DGEBA
07	04		Electron Microscopy	Heterogeneity	MPDA

19. ABSTRACT (Continue on reverse if necessary and identify by block number)

An electron microscopic study of fracture surfaces and microtomed sections of a cured epoxy resin based on a difunctional Bisphenol-A type resin cured with different amounts of metaphenylene diamine is presented. Heterogeneities in the 5-100 nm range are seen to be present and have relatively higher crosslink density compared to the surrounding matrix. It is observed that the fracture path is around the heterogeneity and not through it. The size of the heterogeneity is a function of the curing agent concentration and also of the cure cycle. The stoichiometric sample, which has the highest crosslink density and the highest glass transition temperature, has the smallest heterogeneities. On either side of stoichiometry, the heterogeneity size increases. The samples subjected to a more severe postcuring cycle have much larger heterogeneities. The possible physical basis for these differences is discussed.

20. DISTRIBUTION/AVAILABILITY OF ABSTRACT UNCLASSIFIED/UNLIMITED ☐ SAME AS RPT. ☒ DTIC USERS ☐	21. ABSTRACT SECURITY CLASSIFICATION Unclassified
22a. NAME OF RESPONSIBLE INDIVIDUAL W. W. Adams	22b. TELEPHONE NUMBER (Include Area Code) 513-255-9148 22c. OFFICE SYMBOL AFWAL/MLBP

DD FORM 1473, 83 APR EDITION OF 1 JAN 73 IS OBSOLETE.

11. Morphology of Cured Epoxy Resin

FOREWORD

This report was prepared by the Polymer Branch and the Mechanics and Surface Instructions Branch of the Nonmetallic Materials Division and Systems Research Laboratories under Contract Number F33615-83-C-5073. The work was initiated under Project No. 2303, "Research to Define the Structure Property Relationships," Task No. 2303Q3 Work Unit Directive 2303Q307, "Structural Resins." Dr. Thaddeus E. Helminiak served as the AFWAL/ML Work Unit Scientist. Co-authors were: V. B. Gupta, National Research Council Senior Resident Research Associate, L. T. Drzal (AFWAL/MLBM), W. W. Adams (AFWAL/MLBP), and R. Omlor, Systems Research Laboratories.

This report covers research conducted from July 1982 to June 1984.

The authors are grateful to Dr. Y. L. Chen and Mr. R. Bacon for assistance with the SEM, Ms. P. Lloyd for microtomy, Mr. Dolf Bierman for plasma-etching, Ms. Mary K. Hershey for the FTIR osmium-tetroxide reactivity study, and Dr. S. Kumar for size measurement studies. One of the authors (V. B. Gupta) is grateful to the Air Force Systems Command and the National Research Council, Washington, DC, for the award of an Associateship during 1982-84 and to the Indian Institute of Technology, New Delhi for the grant of leave.

1. INTRODUCTION

The morphology of a number of cured epoxy resin systems has been studied by electron microscopy and considerable evidence has been obtained for the existence of heterogeneities at the 5-100-nm size level.[1-11] These heterogeneities have been shown to be regions of high crosslink density in a matrix of relatively lower crosslink density. Oberlin et al.[1] studied ultramicrotomed 40-nm-thick sections of a cured epoxy resin system with the electron microscope column under "clean" vacuum obtained by ionic pumping and imaged, what they claimed to be, single molecules of the epoxy resin used. At vacuum levels used in the normal microscopes, viz. 10^{-4} to 10^{-5} torr, "nodules" of 10 nm size having a local order higher than that of the bulk became visible. It was therefore concluded that freshly prepared resin is homogeneous and remains stable while under study in a clean vacuum. In poorer vacuum, electron irradiation etches the sample and inhomogenetities develop. Aspbury and Wake[2] studied ultramicrotomed sections of some other epoxy systems which were shadowed with platinum-carbon. They identified the basic nodular feature to be of about 5 nm size but found that aggregates of nodules 10 to 40-nm size were by far the most notable features of the electron micrographs. Studies on the morphology of cured epoxy systems as a function of curing agent concentration have been made using etched surfaces and fracture surfaces or their replicas, and heterogeneities in the 10-60 nm size range have been identified; their sizes depended strongly on the curing agent concentration.[3-7] However, while Racich and Koutsky[3,4] and Mijovic and Koutsky[5] concluded that lower stoichiometries had entities of larger size, Manson et al.[6] and

Misra et al[7] found that higher stoichiometries had larger heterogeneities. Bell[8] and Takahama and Geil[9] have also shown that heterogeneities of 10-50 nm size exist in cured epoxy resins. Morgan and O'Neal present evidence[10] for 8-9 nm size heterogeneities which aggregate into larger entities. Bell has additionally shown[8] that the degree of mixing of the reactants can affect the homogeneity of the cured resin system and the size of the heterogeneity would therefore be a function of the degree of mixing.

In addition to electron microscopy, the existence of heterogeneities has also been inferred from studies based on various other techniques.[12-15] Electron paramagnetic resonance (EPR) studies on cured epoxy resin have given evidence[12,13] for two phases, and it was shown that solvents are preferentially sorbed in the low crosslink regions which have greater free volume content. Nuclear magnetic resonance (NMR) studies of epoxy resins[13] have shown the existence of mobile and rigid regions, and the size of the rigid regions has been found to be in the 22-46-nm range. Matyi, Uhlmann and Koutsky [14] found evidence for inhomogeneities in the size range of 10-100 nm, with the most frequent size range being 10-20 nm by small-angle x-ray scattering. They stated that the heterogeneities could either be regions which differ in crosslink density or could be gas bubbles. Kriebich and Schmid showed [15] that annealing can cause phase separation of the high and low crosslinked phases, and this results in a splitting of the glass transition temperature. Such an effect could, however, also arise from a transient phase due to aging.[16]

The nonuniformity of crosslink density can have important consequences on the properties of the cured epoxy resin. Therefore

there has been considerable interest in studying the origin of the heterogeneities in these systems. But it is still not clear why, when, and how they form. Extremely divergent views have been expressed. Funke states[17,18] in a discussion of the reaction mechanisms leading to the formation of crosslinked systems that the formation of homogeneous networks represents an exception in crosslinking polymerization. A similar conclusion was reached by Labana et al.[19] Lunak and Dusek[20] and Dusek et al.[21] on the other hand, have postulated that epoxies are more likely to have a homogeneous structure. Deanin has described[22] how inhomogeneities may form during crosslinking of an initially homogeneous resin. When a reactive polyfunctional low molecular weight monomer reacts with a crosslinking agent, the statistical probability of forming each new bond is equally probable throughout the material. When molecular weight has grown to a certain critical size, the molecule is no longer small enough to remain uniformly dispersed in the liquid medium by Brownian motion and begins to segregate out in the form of a rubbery gel. With further reaction within this segregated mass, the amount of available reacting species in the neighborhood is reduced. The final cured product contains highly crosslinked particles separated by relatively weakly bound interfacial areas. Bobaleck et al.[23] Solomon[24] and Labana et al.[19] have suggested that the two-phase system is produced before the formation of the macrogel. Apicella et al have postulated[25] that inhomogeneous networks form during postcuring. Stevens et al[26] investigated local order in unreacted DGEBA epoxy monomer by Rayleigh scattering and Brillouin spectroscopy and showed that aggregates of 20-70 nm size were present in the resin and were caused by differences in intermolecular hydrogen bonding which was

related to the epoxide/hydroxyl ratio of the resins. They suggested that this local order in the unreacted resin could promote inhomogeneous reaction and lead to network inhomogeneity. Luttgert and Bonart[27] have postulated that the size of the heterogeneity in the cured resin depends on the rate of microgel formation or nucleation and the rate of growth of the gel particles. At high curing temperatures, the rate of nucleation will be fast and the great number of microgels formed permits growth only to a small size. Low curing temperatures initiate only a small number of gel particles, and the cured resin will show large globular heterogeneities.

In the present investigation, the cured epoxy resin system studied was based on diglycidyl ether of Bisphenol-A (DGEBA) which was cured with different amounts of metaphenylene diamine (mPDA) under two curing cycles. The studies included transmission electron microscopy (TEM), scanning electron microscopy (SEM), and scanning transmission electron microscopy (STEM) of unetched and etched fracture surfaces and their replicas and of the unstained and stained microtomed sections. Heterogeneities in the 5-100 nm range were found to be the predominant feature and their size was a function of the curing agent concentration and cure history. Broadly speaking, the size was the smallest for the sample containing stoichiometric amount of curing agent and increased on either side of stoichiometry. The size of the heterogeneity also showed considerable increase on postcuring. Possible reasons for these are discussed.

2. EXPERIMENTAL METHODS

The epoxy resin used was Epon 828 (Shell) which is based on DGEBA and has the following chemical structure:

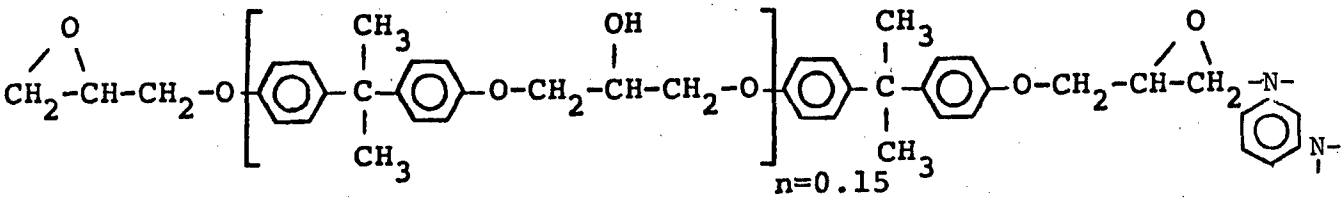

It is a liquid of high viscosity at room temperature with an epoxide equivalent of 190. The curing agent used was metaphenylene diamine (mPDA), an aromatic amine which is a solid at room temperature with a melting point of 68°C. It has the following chemical structure:

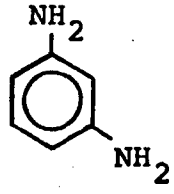

The epoxy molecule has two epoxy groups while the curing agent has four active hydrogens. For all the epoxide groups to react, 14.5 parts by weight of mPDA per 100 parts by weight of Epon 828 are required; this is the stoichiometric amount of curing agent. In the present investigation, the resin was cured with 7.5, 10, 14.5, 20, and 25 phr of curing agent.

The resin and the curing agent were heated in separate containers in an oven set at 75°C. When the mPDA had melted completely, it was mixed with the epoxy resin and then degassed under vacuum for seven minutes. Degassing removes the air bubbles and at the same time vigorous mixing takes place. The mixture was then cast into rectangular bars, dogbone coupons, and thin discs by pouring into flexible silicone rubber molds which were open at the top. The curing cycle used was two hours at 75°C followed by two hours at 125°C. The oven was then switched off and the cured samples allowed to cool within the oven until they reached room temperature; this took about four hours. These samples will be designated as "standard cure." Another set of samples was prepared by postcuring the standard-cure samples at 175°C for six hours in inert gas environment; they will be referred to as the "postcured" samples. While detailed studies were conducted on the standard-cure samples, only limited amount of work was done on the postcured samples.

A notch was made on the narrowest side of the rectangular specimen with a rotating cutter and the crack so formed was gently touched under slight pressure with a fresh razor blade. The two ends of the sample were held with pliers and immersed in liquid nitrogen. The sample was taken out from the liquid nitrogen bath after sometime and then immediately fractured by bending around the notch. Some of the fracture surfaces were etched for 30 minutes in an argon plasma using 50 watts power at about 20 ml/mil flow of argon gas and a 0.5 mm mercury pressure using an International Plasma Corporation unit. The temperature inside the plasma unit was measured with a thermocouple and after 30 minutes was found to be 65°C. The as-fractured and

plasma-etched fracture surfaces were coated with gold-palladium on a sputtering unit, and the coated surfaces were examined on an ETEC Autoscan scanning electron microscope and on the JEOL scanning transmission electron microscope in the scanning mode.

It has been shown[28] that the usual method of preparing replicas of epoxy surfaces, viz. the use of polyacrylic acid as the replicating fluid can give rise to artifacts. Hence a modified replication technique was developed and used.[29] The replicas were examined on a JEOL 100CX scanning transmission electron microscope in the transmission mode.

Some studies were also made on plasma-etched as-cured surfaces of the standard-cure samples in the SEM and on their replicas in the TEM.

Microtomed sections were prepared by cutting thin sections of standard-cure samples on an Ultracut, Reichert ultramicrotome using a diamond knife at room temperature. Though the thickness of the microtomed sections was not measured, it was expected to be in the 50 nm range. Some of the sections were mounted on unsupported fine nickel grids and stained in 10 percent osmium-tetroxide in benzene and allowed to dry at room temperature. Some dilute solution infrared analysis was conducted to determine the location of the osmium-tetroxide reaction. Results from this study showed that primary and secondary amines were attacked by osmium-tetroxide but that tertiary amines were not. It was therefore suspected that incompletely reacted amine sites, which will be present in relatively greater quantity in the low crosslink density matrix phase, will be preferentially stained. The stained sections were examined on an optical microscope, and they showed quite uniform staining; the amine-excess samples were relatively darker. The stained

sections were then examined on the SEM and STEM. An energy-dispersive x-ray scan of this sample for osmium was made.

3. RESULTS AND DISCUSSION

From the initial exploratory work, it was quite clear at the outset that the fracture surfaces of cured epoxy resin samples contained inhomogeneities in the 5-100 nm range. The relative merits of the various techniques of sample preparation were therefore evaluated in relation to the clarity with which they revealed the underlying structure in a reproducible manner. The samples included as-cured surfaces etched for 90 minutes in cold argon plasma, unetched and 30 - minute plasma-etched fracture surface, 30-minute boiling acetone-etched fracture surfaces, unstained and stained microtomed sections with uranyl acetate and osmium-tetroxide as the staining agents. While all these techniques revealed the presence of heterogeneities, the plasma-etched fracture surfaces and the osmium-tetroxide stained ultramicrotomed sections gave the most satisfactory and reproducible results. Among the examination techniques, use was made of SEM, TEM, and STEM.

3.1 Plasma-Etched Fracture Surfaces

The fracture surfaces of the standard-cure samples etched with a cold argon plasma for 30 minutes were first examined on the ETEC Autoscan scanning electron microscope. The scanning micrographs of the fracture surfaces of samples with the five stoichiometries are shown in Figures 1(a) to (e). The heterogeneous morphology is distinctly visible, and there are differences in the size and size distribution of

the heterogeneities in the five samples. From enlarged photographs, the sizes of about 200 entities were measured; in all cases they were found to fit a log normal distribution and are shown in Figure 2 as linear plots of size on a log-probability scale. The median value at 50 percent cumulative frequency was taken as the average size of the heterogeneity. The variation of the average size with curing agent concentration is shown in Figure 3. The stoichiometric sample, which has the maximum crosslink density and the maximum Tg (30), has the smallest heterogeneity. On either side of stoichiometry, the heterogeneity size increases as crosslink density and Tg decrease.

The plasma-etched fracture surfaces of the postcured samples were next studied on the JEOL 100CX STEM in the scanning mode. The scanning micrographs for the five stoichiometries are shown in Figures 4(a) to (e). Distinct heterogeneous morphology is seen and the heterogeneities are now larger in size. No detailed size distribution studies were made on these micrographs, but it appeared that in these samples the sizes were larger by a factor of about 2 to 3 relative to the standard-cure samples. Also the stoichiometric sample still had the smallest size heterogeneity. Possible reasons for this increase in heterogeneity size on postcuring will be discussed later.

Dusek et al studied[21] the fracture surfaces of two amorphous thermoplastic polymers, viz. polystyrene and polymethylmethacrylate along with those of cured epoxy resin by electron microscopy. They used an air plasma to etch the fracture surface and observed inhomogeneities of 20-40 nm size in all the samples. Since amorphous polystyrene and polymethylmethacrylate are believed to be homogeneous, the authors concluded that the inhomogeneous structure is not an inherent property

of the cured epoxy resins and apparently the effects that are seen are artifacts resulting from plasma-etching. It was therefore considered worthwhile to study the fracture surfaces of these amorphous thermoplastics when etched with an argon plasma. A thin sheet of atactic polystyrene was melt-pressed from polystyrene of molecular weight 200,000 and Mw/Mn close to unity, supplied by Pressure Chemical Co., Pittsburgh, Pennsylvania, USA. This and a commercial "Plexiglas" sheet (Rohm and Haas, USA) were then fractured in liquid nitrogen and etched with argon plasma under the same conditions as used for the epoxy specimen. As shown in Figures 5(a), (b) and (c), the low magnification scanning micrographs of the fracture surfaces indicate that there is extensive plastic deformation in the amorphous thermoplastics but not in the epoxy sample. At higher magnification, the amorphous thermoplastics are relatively featureless as shown in Figures 5(c) and (d), but the epoxy sample (Figure 5(e)) shows heterogeneities in the 5-50 nm range. Thus the heterogeneities in the plasma-etched epoxy fracture surfaces may not be an artifact. The experiments of Dusek et al.[21] differed from those reported here in two respects: first, they used an air and not an argon plasma; and second, they studied a replica of the fracture surface using polyvinyl alcohol in water as the replicating agent and not the fracture surface itself. It would be interesting to find out if these factors resulted in introducing the artifacts.

The existence of heterogeneous morphology in all the samples was confirmed by using a modified replication technique,[29] which involved the coating of the fracture surface with a thin film of carbon before replication. As an illustration, the transmission micrograpy of the replica of the 30-minute plasma-etched fracture surface of the

stoichiometric sample is shown in Figure 6 along with the scanning micrograph of the fracture surface at a similar magnification for comparison. The heterogeneities are quite well resolved in the replica micrograph, and their size distribution and average size are quite close to those obtained from the earlier data.

3.2 Plasma-Etched As-Cast Surface

It has been stated that the fracture process itself can introduce the types of features that are being observed, viz. spherical entities in the 5-100 nm range.[31] The as-cured surface of the stoichiometric sample plasma-etched for 90 minutes was therefore studied on the SEM and its replica on the STEM in the transmission mode. As shown in Figures 7(a) and (b), a network of interconnected inhomogeneities is distinctly seen on the as-cast surface. The size of the heterogeneity is consistent with the earlier data obtained from the fracture surfaces. Detailed studies on samples of different stoichiometry showed that the results were not always reproducible. A likely reason for this is that the as-cured surface, which was exposed to air during curing, could lose some amine and thus have a morphology which is not representative of the bulk.

3.3 Microtomed Sections

The as-microtomed sections of the standard cure sample containing stoichiometric amounts of curing agent were examined on the STEM in the transmission mode, and a series of through-focus micrographs were taken. As shown in Figure 8, which is the in-focus micrograph, heterogeneities in the 5-30 nm size range are seen; however, they are not very distinct. The microtomed sections of atactic polystyrene were similarly examined, and the through-focus series of micrographs (Figure 9) show a rather

featureless surface and do not reveal any recognizable morphological entities. The as-microtomed section of the standard-cure sample containing the stoichiometric amount of curing agent was shadowed with carbon-platinum, and as shown in Figure 10, entities of 5-20 nm size can be seen on the surface. Such shadowing did not bring out any structure in atactic polystyrene.

Next, the microtomed sections stained with osmium-tetroxide were examined on the STEM in the transmission and scanning transmission modes. As stated earlier infrared studies had shown that the osmium-tetroxide attacks the primary and secondary amines. Since there would be more unreacted amine in the less crosslinked regions, it would be expected that the boundaries around the heterogeneities will be stained to a relatively higher degree and thus would appear dark in the micrographs. However, since the thickness of the sections examined is at least twice the heterogeneity size, the entities in the path of the electron beam will overlap and distinct boundaries would not be expected to show. The micrograph shown in Figure 11(a) for the standard-cure, 14.5 phr sample shows reasonably distinct boundaries of entities indicated by arrows. To emphasize this effect, a low exposure print of the same micrograph is also included (Figure 11(b)) as it defines the boundaries more clearly. The size of the entities is consistent with the earlier data. An energy-dispersive x-ray scan of this sample for osmium showed (Figure 12) that osmium is nonuniformly distributed in the sample in a manner similar to the distribution observed in the TEM and SEM micrographs. A micrograph of an osmium-tetroxide stained sample of different stoichiometry, viz. 25 phr standard-cure sample (Figure 13) also shows dark stained rings around the heterogeneity.

Some authors have suggested[2,10] that the heterogeneities in the 20-60 nm range are aggregates of basic "nodules" of around 5 nm or 8 nm size. In the present studies, the osmium-tetroxide-stained sections, as shown in Figures 11(a) and 13, do indicate that the heterogeneities could indeed be aggregates of smaller entities. However, careful and detailed studies are required to verify this since the size of the smaller entities is close to the size level of statistical noise of the microscope. This work is under consideration.

During investigation of a microtomed section of a sample prepared from X-22 resin, which is a purified form of Epon 828 containing stoichiometric amounts of mPDA, an interesting result was obtained. When this sample was being examined in the electron microscope, beam damage caused two holes in the specimen and this resulted in tearing of the film along the arrows indicated in Figure 14. A 200-nm-wide strip can be seen bridging the advancing tears and is apparently under considerable stress. Under this stress the sample appears to have stretched, and since this part of the section has become thin, the heterogeneities and the dark stained rings around them can be seen more distinctly. A dark band, which at its narrowest is around 5 nm wide, runs through the middle of this strip, and it is clear that rupture is more likely to occur along this band. This dark band is apparently formed as a result of the alignment of the heterogeneities and represents the boundary between them. Close examination of this micrograph shows that the circular features observed in the normal stained thin sections are now elongated into elliptical shapes. From prints of this micrograph at various exposure times, the heterogeneity boundaries could be traced in a number of cases and, as shown in Figure

15, follow the stress field by deforming and/or aligning suitably.

4. THE HETEROGENEITY SIZE

4.1 The Standard-Cure Samples

The data on size distribution and average size of the heterogeneity for the standard-cure samples was presented earlier in Figures 2 and 3. The sample with the stoichiometric amount of curing agent (14.5 phr) has heterogeneities of the smallest size. It has been shown elsewhere[30] that this sample has the highest crosslink density and also the highest glass transition temperature.

The stoichiometric sample has the right proportion of the resin and the curing agent so that each epoxy group has an active amine hydrogen to react with in the reacting mass. Assuming that the resin and the curing agent are well-mixed, the stoichiometric sample will form a network in which, in the ideal case, all the epoxy and amine groups will have reacted. In the other samples there is either an excess of epoxy or of amine, and the cured sample will therefore contain unreacted epoxy or amine groups. Infrared studies reported elsewhere,[30] broadly speaking, confirm these expectations. In an exothermally reacting mass, the greater the temperature rise, the larger the number of nuclei, as postulated by Luttgert and Bonart.[27] Though some attempts were made to monitor the temperature rise during the curing cycle, a consistent picture did not emerge and no comments will therefore be made on this aspect at this stage. The nuclei so formed will continue to grow until the growing network reaches its Tg. Once the network has reached its Tg, the diffusion of the reacting species will be hindered and the reaction will soon be quenched. The Tg data for the standard-cure samples[30] is summarized in Table 1. The data for the postcured samples

are also included in this table since they are required at a later stage. It is noteworthy that the Tg of the standard-cure, stoichiometric sample (145°C) is higher than the final cure temperature (125°C) for this sample. A phenomenological model to explain the heterogeneity size data emerges from this discussion. In the stoichiometric sample, since the reacting mass has the correct proportions of resin and curing agent, network formation is rapid and the approach to a Tg of 145°C is apparently fast. The reaction is quenched at quite an early stage, thus allowing the nuclei to grow only to a small size heterogeneity. In the other samples unreacted groups get incorporated, and the network approaches its Tg rather slowly. Since the Tg's of all these other samples are lower than the final cure temperature, these samples will be in the rubbery state throughout the cure cycle when some form of reaction can continue to take place. The heterogeneities will consequently be larger in size.

4.2 The Postcured Samples

The effect of postcuring on heterogeneity size has not been extensively studied. Yamini and Young[11] report that when samples cured at room temperature for 24 hours were postcured at 100 and 150°C, the size of the heterogeneity decreases dramatically with an increase in the postcuring temperature. Aspbury and Wake,[2] on the other hand, report that when samples which had first been cured at 60°C for four days were postcured at 150°C, the heterogeneity size almost doubled. Our results are similar to those of Aspbury and Wake.[2] For our postcured samples, the Tg data is given in Table 1 and it may be seen that the postcure temperature (175°C) is higher than the sample Tg in all cases.

A phenomenological explanation of the results presented is given below. In the studies of Yamini and Young,[11] the samples were postcured at room temperature for 24 hours. Very limited reaction would have occurred in the samples at this stage. When the samples were postcured at a higher temperature, a large number of nuclei will form at sites which are still unreacted, and the higher the postcuring temperature, the larger the number of nuclei.[27] Also, curing will be more rapid at higher temperature. Thus the heterogeneity size would be expected to decrease with increase in postcuring temperature, as was observed. Aspbury and Wake,[2] on the other hand, first cured the samples at 60°C for four days followed by a postcure at 150°C for eight hours and observed that the heterogeneity size had almost doubled on postcuring. The results in the present investigation followed a cure cycle of 75°C for two hours and 125°C for two hours followed by postcuring of 175°C for six hours. The heterogeneity sizes in the five samples studied increased from 23-45 nm to 68-85 nm on postcuring. In these samples and also in the samples of Aspbury and Wake,[2] considerable reaction had apparently already occurred in the initially-cured samples themselves. Thus on postcuring, though the samples were in a rubberlike state, the number of available unreacted sites will be limited. Thus the new entitites will form as a result of reorganization of the pre-existing heterogeneous morphology of this sample rather than by the formation and growth of new nuclei. However, since the mechanism of reorganization has not been studied, no comments on this aspect can be offered at this stage.

5. CONCLUSIONS

A combination of techniques of sample preparation and of sample examination show that the cured epoxy resin system investigated has a heterogeneous morphology and that the sizes of the spherical entities obtained from these different methods are reasonably consistent. The heterogeneities are entities of higher crosslink density in a matrix of relatively lower crosslink density. The fracture path is around the heterogeneity and not through it. Rapid curing results in small heterogeneities in the stoichiometric sample. In other samples which contain an excess of epoxy or amine, relatively slower curing apparently results in larger heterogeneities. The increase in heterogeneity size on postcuring has been attributed to reorganization of the pre-existing entities.

REFERENCES

1. A. Oberlin, J. Ayache, M. Oberlin, and M. Guigon, J. Polym. Sci., Polym. Phys. Ed., 20, 579 (1982).

2. P. J. Aspbury and W. C. Wake, The British Polymer J., 11, 17 (1979).

3. J. L. Racich and J. A. Koutsky, in "Chemistry and Properties of Crosslinked Polymers," Ed. S. S. Labana, Academic Press, Inc., New York, 1977.

4. J. L. Racich and J. A. Koutsky, J. Appl. Polymer Sci., 20, 2111 (1976).

5. J. Mijovic and J. A. Koutsky, Polymer, 20, 1095 (1979).

6. J. A. Manson, L. H. Sperling, and S. L. Kim, "Influence of Crosslinking on the Mechanical Properties of High Tg Polymers," Technical Report AFML-TR-77-109, July 1977.

7. S. C. Misra, J. A. Manson, and L. H. Sperling, "Network Morphology and Mechanical Behavior of Epoxies," in "Epoxy Resin Chemistry", Ed. R. S. Bauer, ACS Symp. Series 114, American Chemical Society, 157 (1979).

8. J. P. Bell, J. Appl. Polym. Sci., 27, 3503 (1982).

9. T. Takahama and P. H. Geil, Die Makromol. Chemie, Rapid Comm., 3, 389 (1982).

10. R. J. Morgan and J. E. O'Neal, J. Mat. Sci., 12, 1966 (1977).

11. S. Yamini and R. J. Young, J. Mat. Sci., 15, 1823 (1980).

12. I. M. Brown and T. C. Sandreczki, Polymer Preprints, 23, 199 (1982).

13. I. M. Brown, A. C. Lind, and T. C. Sandreczki, "Magnetic Resonance Studies of Epoxy Resins," McDonnell Douglas Research Labs, St. Louis, Missouri, USA, Report No. MDCQ 0721.

14. R. J. Matyi, D. P. Uhlmann, and J. A. Koutsky, J. Polym. Sci., Polym. Phys. Ed., 18, 1053 (1980).

15. V. T. Kreibich and R. Schmid, J. Polym, Sci., Symp. No. 53, 177 (1975).

16. E. S. W. Kong, "Composites Technology Review," 4, 97 (1982).

17. W. Funke, Chimia, 22, 111 (1968).

18. W. Funke, W. Beer, and V. Seitz, Progr. Colloid & Polym, Sci., 57, 48 (1975).

19. S. S. Labana, S. Newman, and A. J. Chompff, in "Polymer Networks," Ed. A. J. Chompff and S. Newman, Plenum Press, 453,(1971).

20. S. Lunak and K. Dusek, J. Polym. Sci., Symp. No. 53, 45 (1975).

21. K. Dusek, J. Plestil, F. Lednicky, and S. Lunak, Polymer, 19, 393 (1978).

22. R. D. Deanin, "Polymer Structure, Properties, and Applications," Cahners Books, Division of Cahners Publishing Co., Inc., Boston, Mass., USA, 354,(1972).

23. E. G. Bobalek, E. R. Moore, S. S. Levy, and C.C. Lee, J. Appl. Polym. Sci., 11, 1593 (1967).

24. D. H. Solomon, J. Macromol. Sci., (Rev.), C-1 (1), 179 (1967).

25. A. Apicella, L. Nicolais, and J. C. Halpin, 28th National SAMPE Symposium on "Materials and Processes - Continuing Innovations," 518, (1983).

26. G. C. Stevens, J. V. Champion, and P. Liddell, J. Polym. Sci., Polym. Phys. Ed., 20, 327 (1982).

27. K. E. Luttgert and R. Bonart, Prog. Colloid and Polym. Sci., 64, 38 (1978).

28. M. D. Skibo, R. W. Hertzberg, and J. A. Manson, J. Mat. Sci., 11 479 (1976).

29. V. B. Gupta, L. T. Drzal, and R. Omlor, Proc. 41st Annual Meeting of the Electron Microscopy Society of American, Ed. G. W. Bailey 36, (1983).

30. V. B. Gupta, L. T. Drzal, C. Y-C. Lee, and M. J. Rich, submitted for publication.

31. R. N. Haward and I. Brough, Polymer, 10, 724 (1969).

TABLE 1

GLASS TRANSITION TEMPERATURE DATA AS OBTAINED FROM DSC

Stoichiometry (phr of mPDA)	Glass Transition Temperature (°C)	
	Standard-Cure	Postcured
7.5	55	71
10.0	76	134
14.5	145	160
20.0	116	120
25.0	95	102

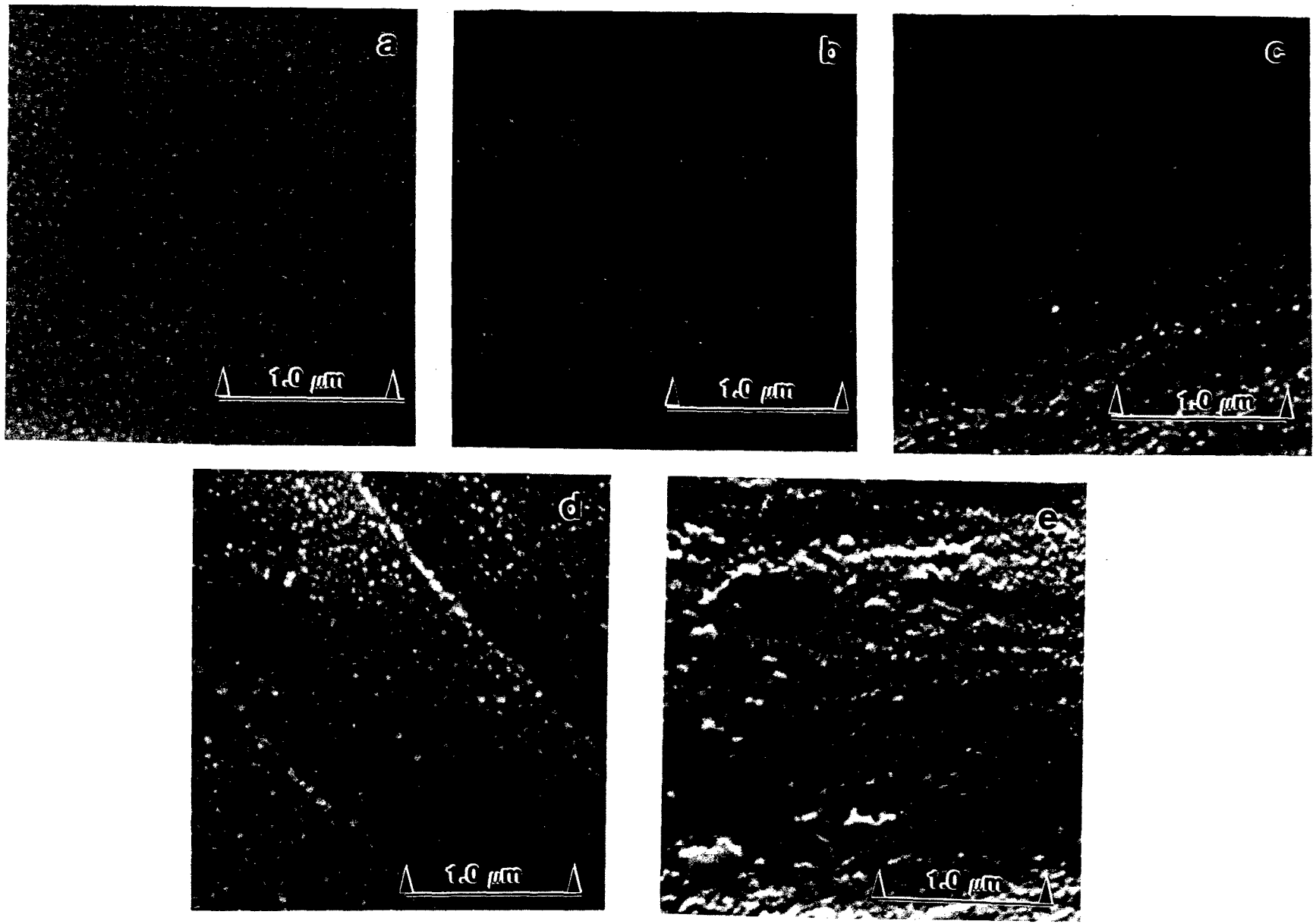

Fig. 1 Scanning electron micrographs of plasma-etched fracture surfaces of standard-cure samples: (a) 7.5 phr, (b) 10 phr, (c) 14.5 phr, (d) 20 phr, (e) 25 phr.

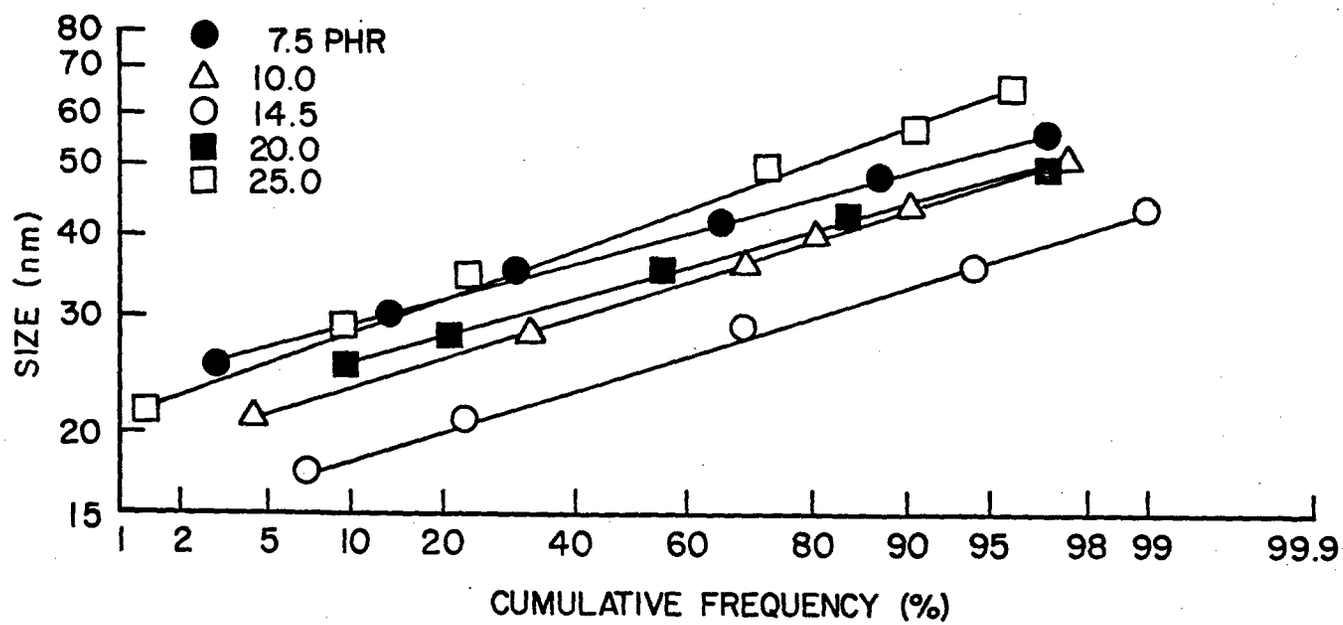

Fig. 2 Size distribution of heterogeneities of the standard-cure samples containing different amounts of curing agent.

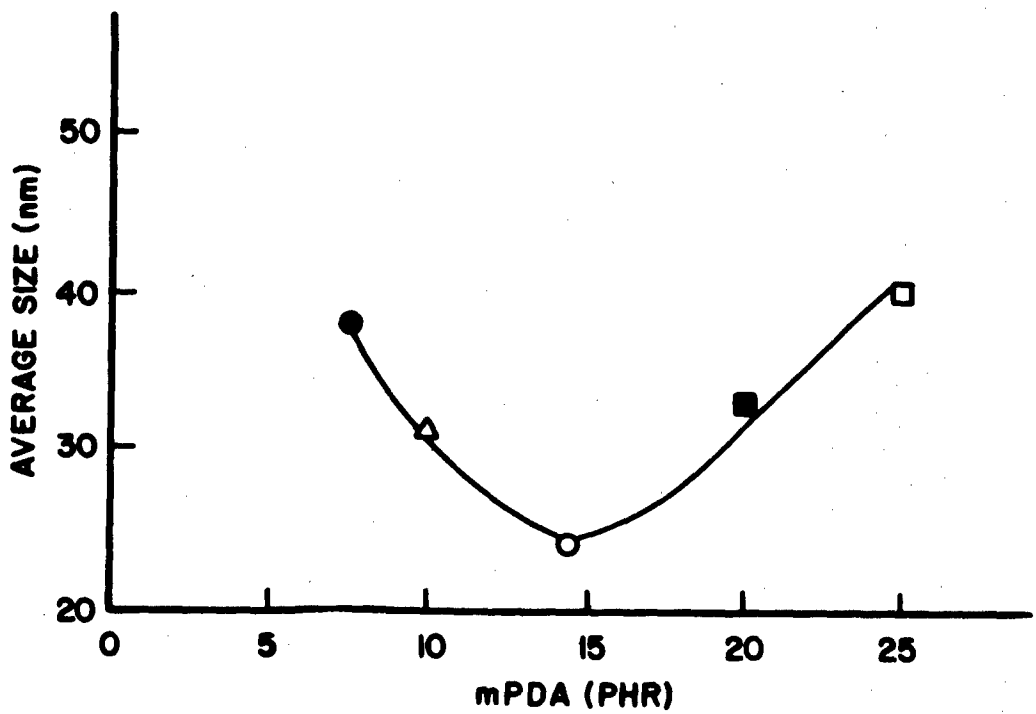

Fig. 3 Variation of the average size of the heterogeneities of the standard-cure samples with curing agent concentration.

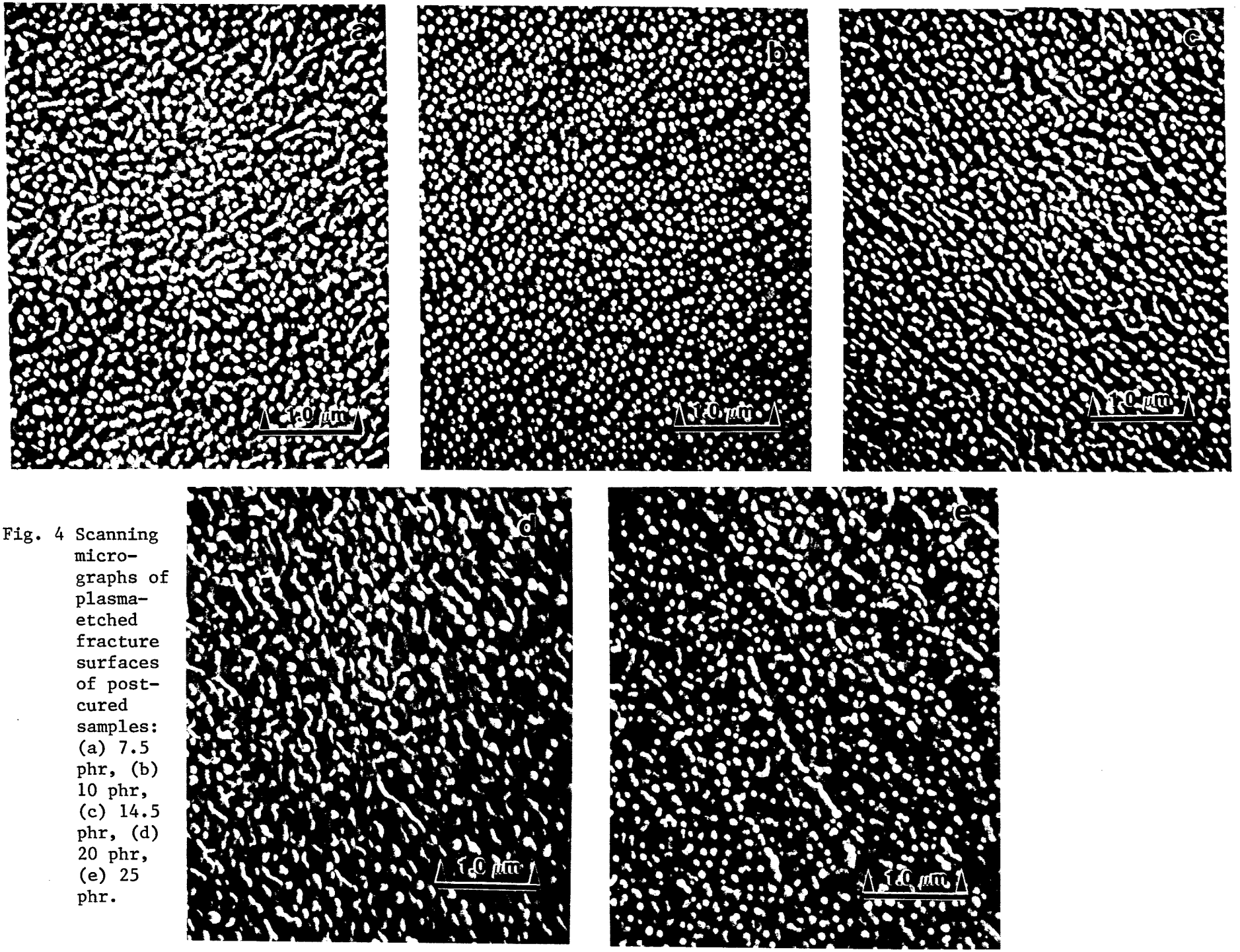

Fig. 4 Scanning micrographs of plasma-etched fracture surfaces of post-cured samples: (a) 7.5 phr, (b) 10 phr, (c) 14.5 phr, (d) 20 phr, (e) 25 phr.

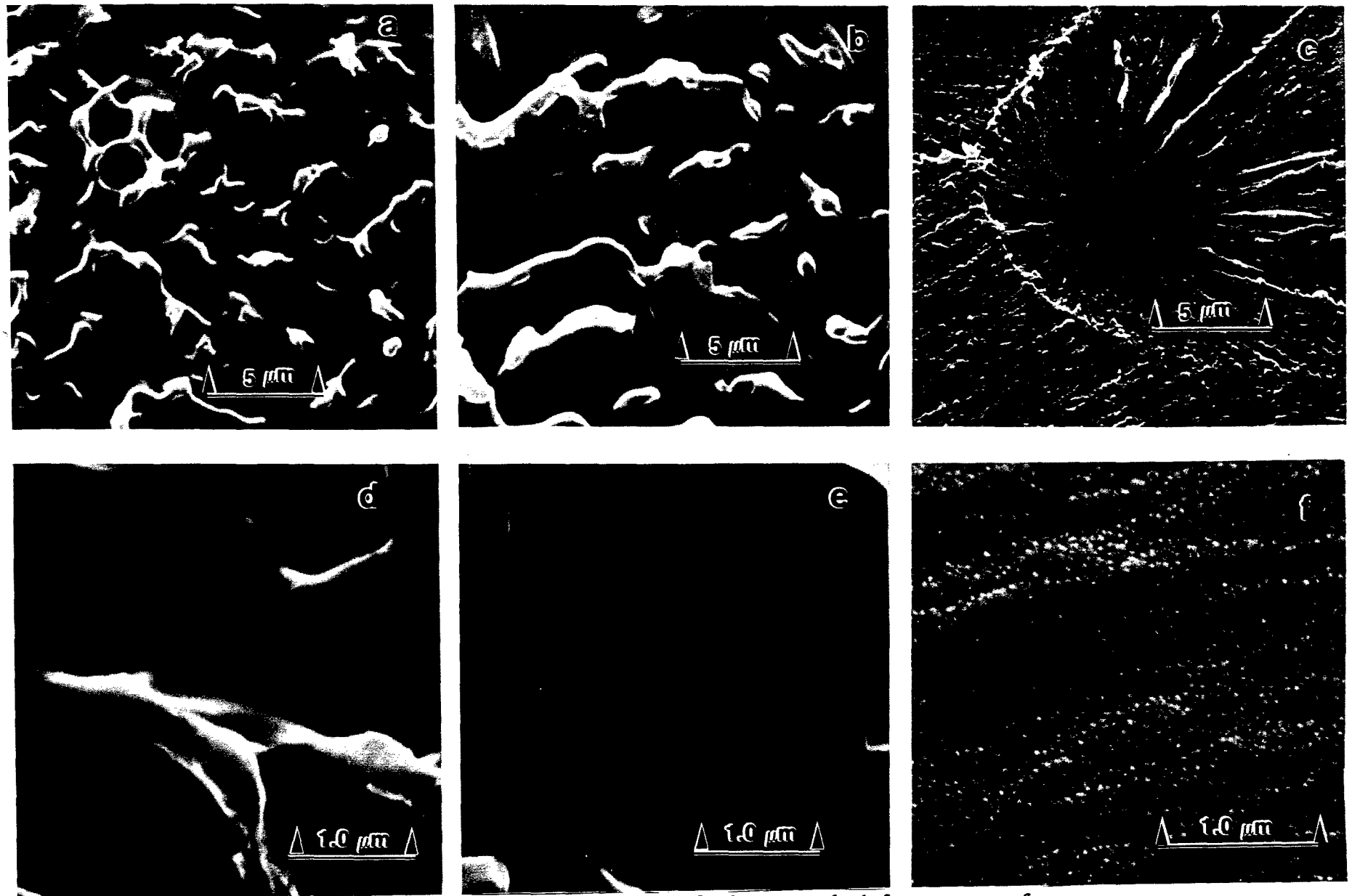

Fig. 5 Scanning micrographs of plasma-etched fracture surfaces at low magnification: (a) PMMA, (b) atactic polystyrene, (c) standard-cure epoxy resin with 10 phr mPDA, and at high magnification, (d) PMMA, (e) atactic polystyrene, and (f) standard-cure epoxy resin with 10 phr mPDA.

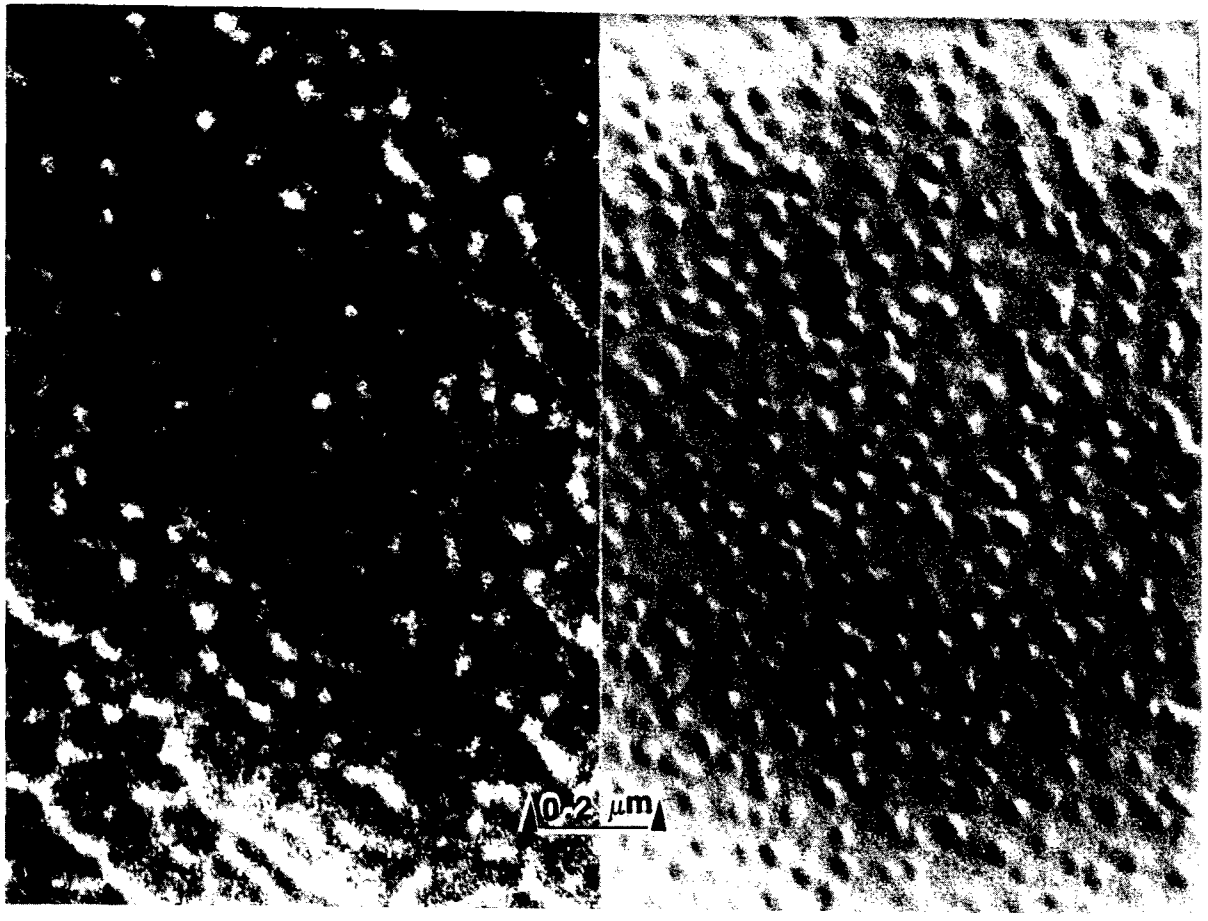

Fig. 6 Micrographs of fracture surfaces of plasma-etched standard-cure stoichiometric samples: (a) scanning micrograph, (b) transmission micrograph of the replica.

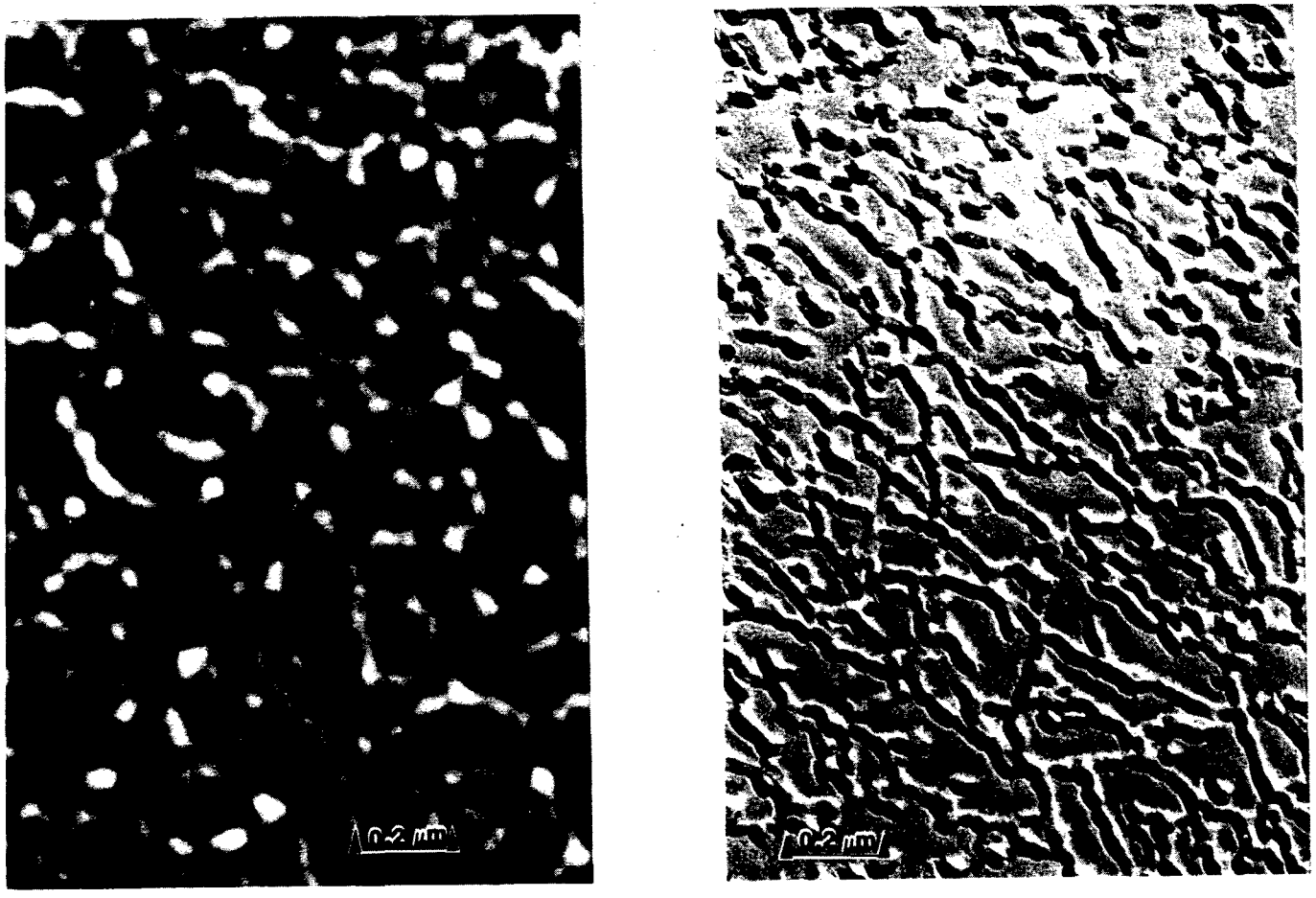

Fig. 7 Micrographs of plasma-etched as-cured surface of the standard-cure stoichiometric sample: (a) scanning micrograph, (b) transmission micrograph of replica.

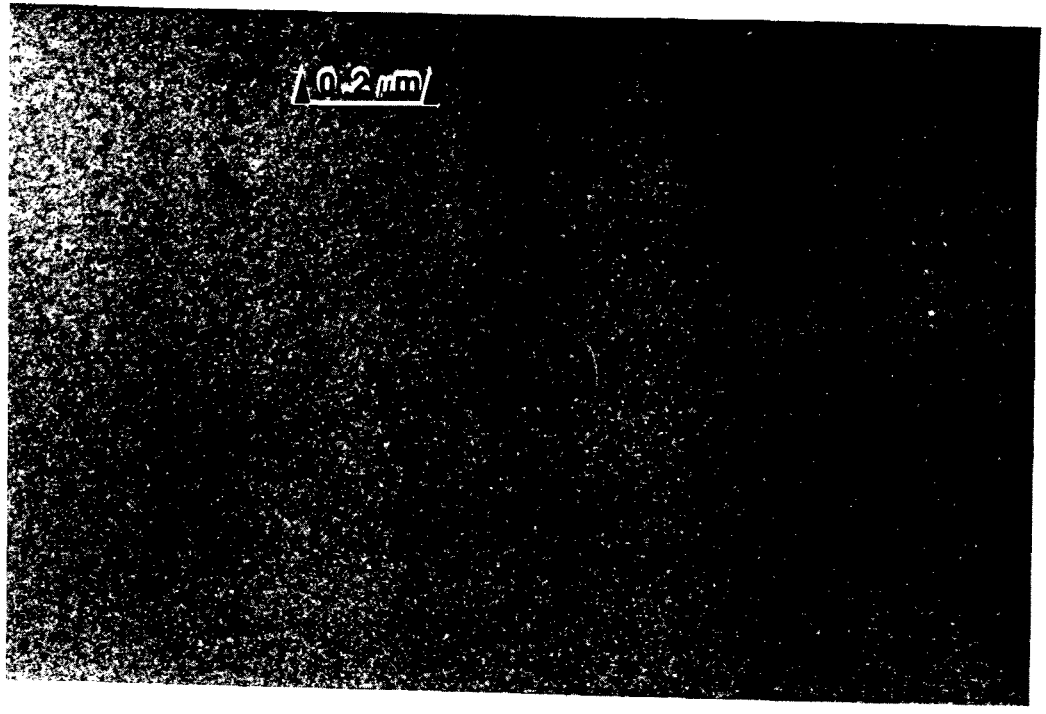

Fig. 8 Transmission micrograph of ultramicrotomed section of standard-cure stoichiometric sample.

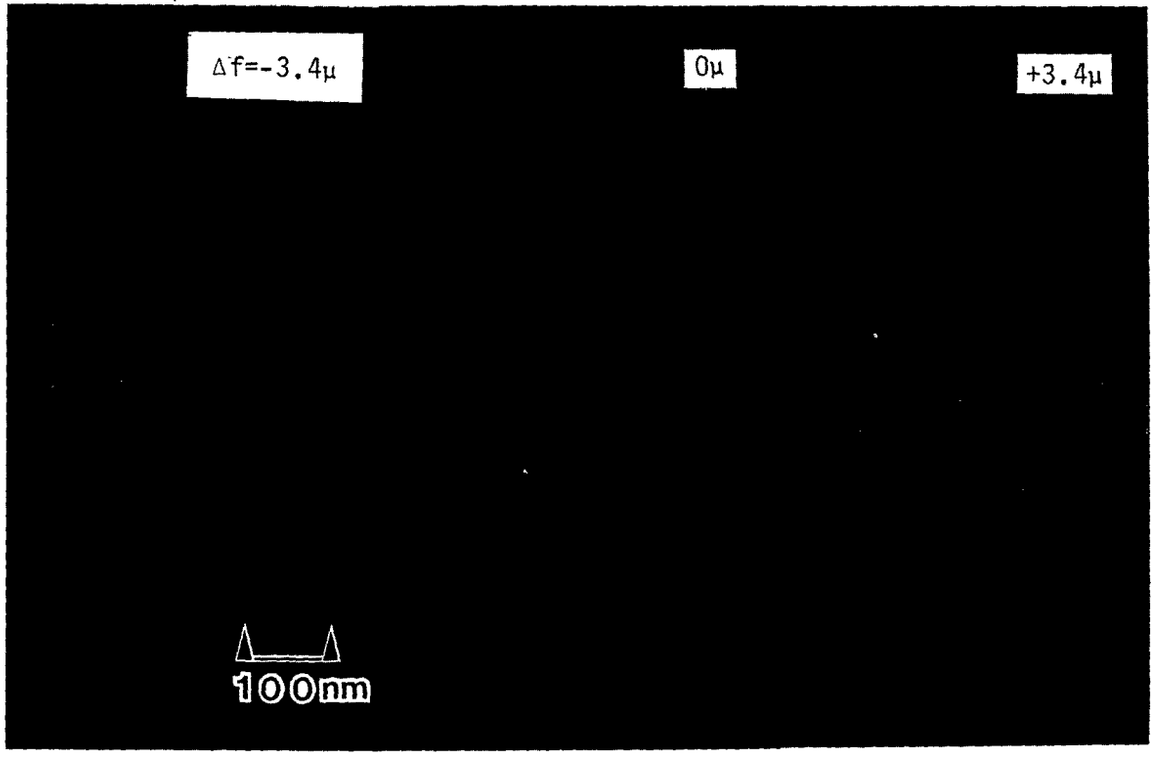

Fig. 9 Transmission micrographs of ultramicrotomed section of atactic polystyrene: through-focus series.

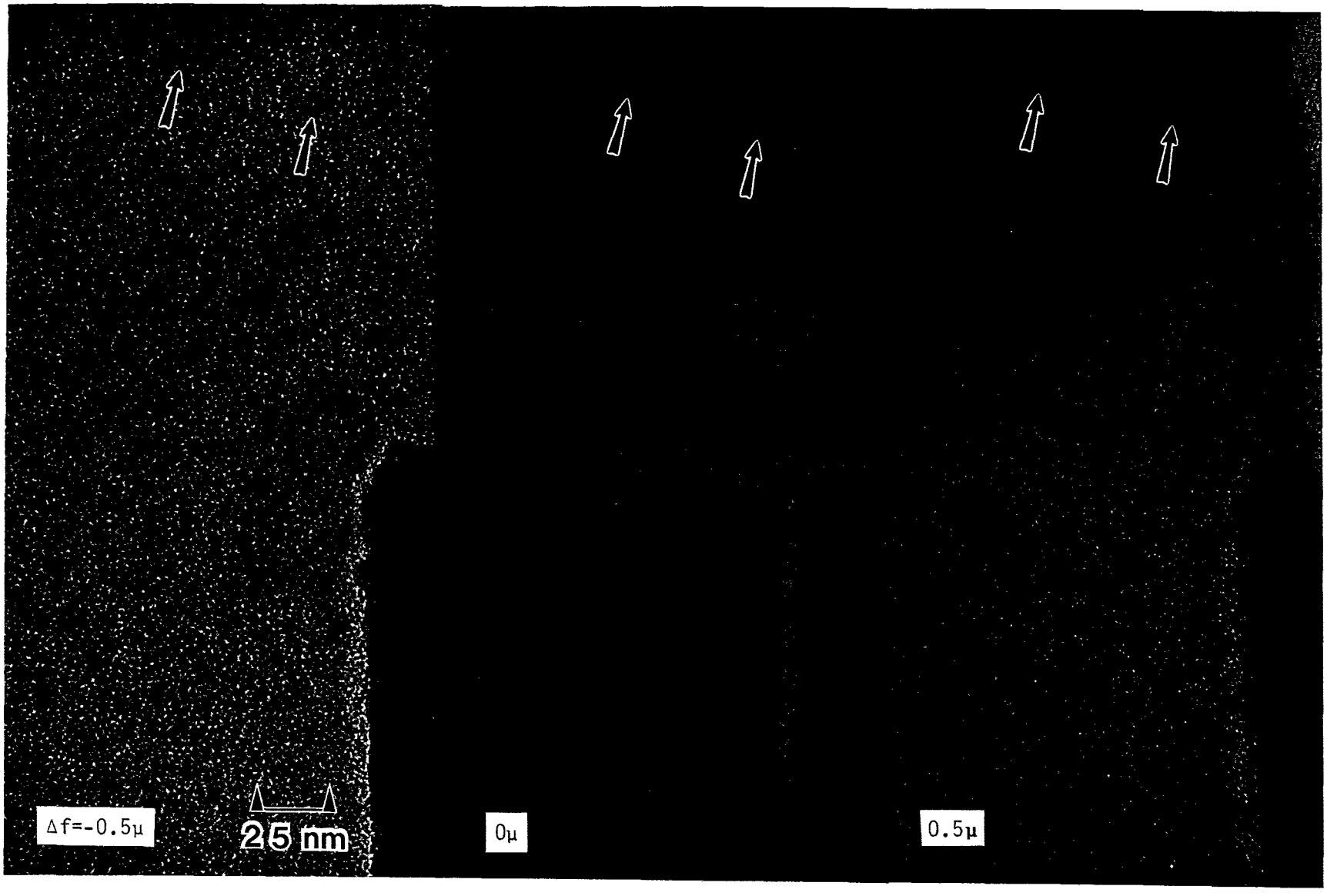

Fig. 10 Transmission micrographs of C-Pt shadowed ultramicrotomed section of standard-cure stoichiometric sample: through-focus series.

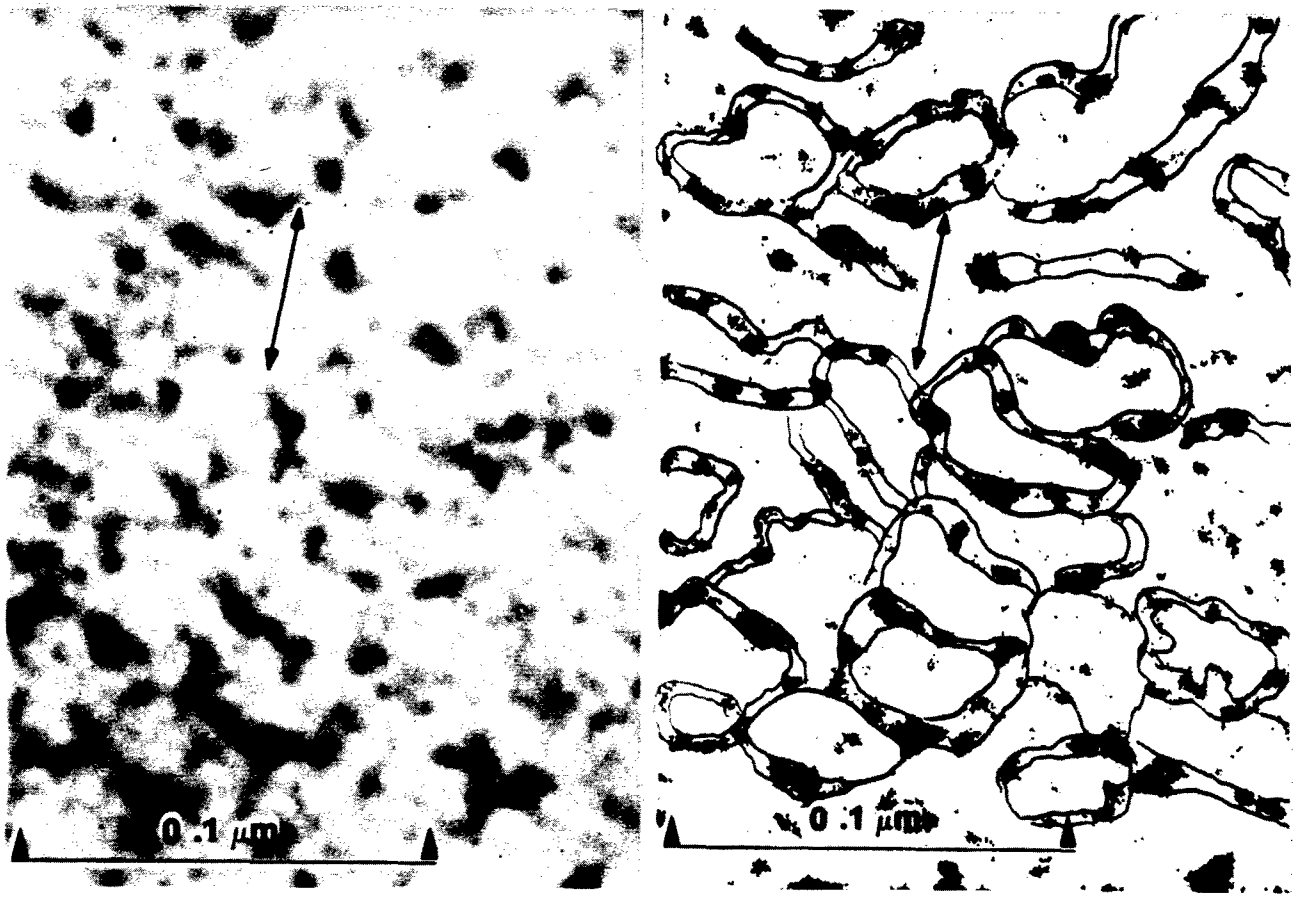

Fig. 11 (a) Transmission micrograph of osmium-tetroxide stained standard-cure stoichiometric sample; (b) The same micrograph printed with a different exposure time.

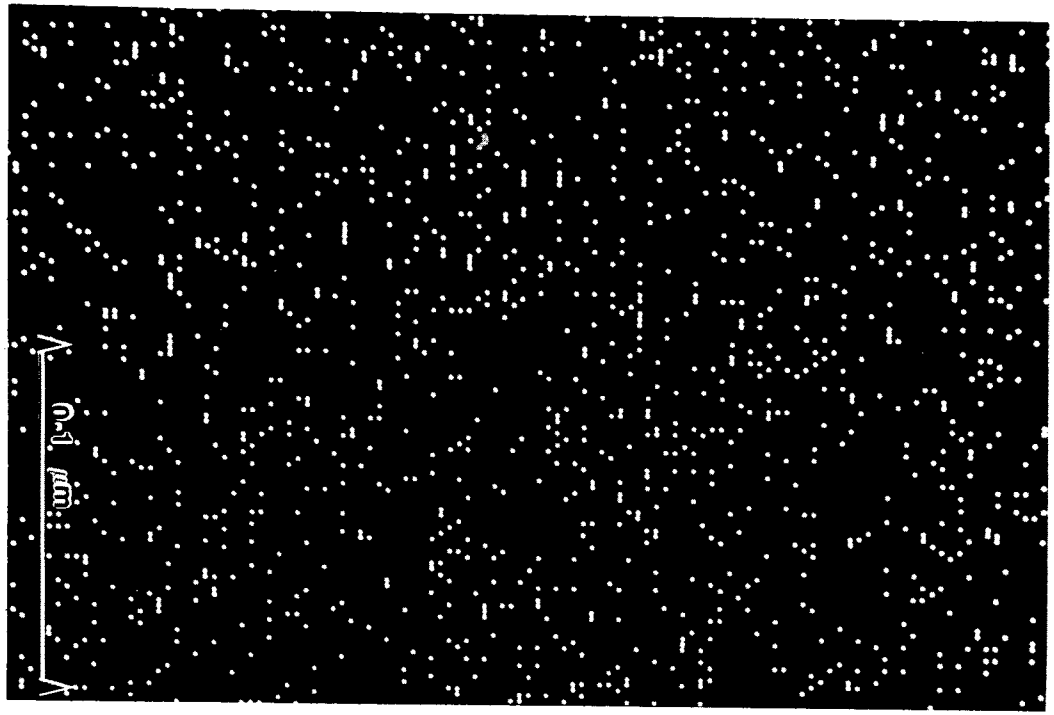

Fig. 12 Energy dispersive x-ray scan of the standard-cure stoichiometric sample for osmium.

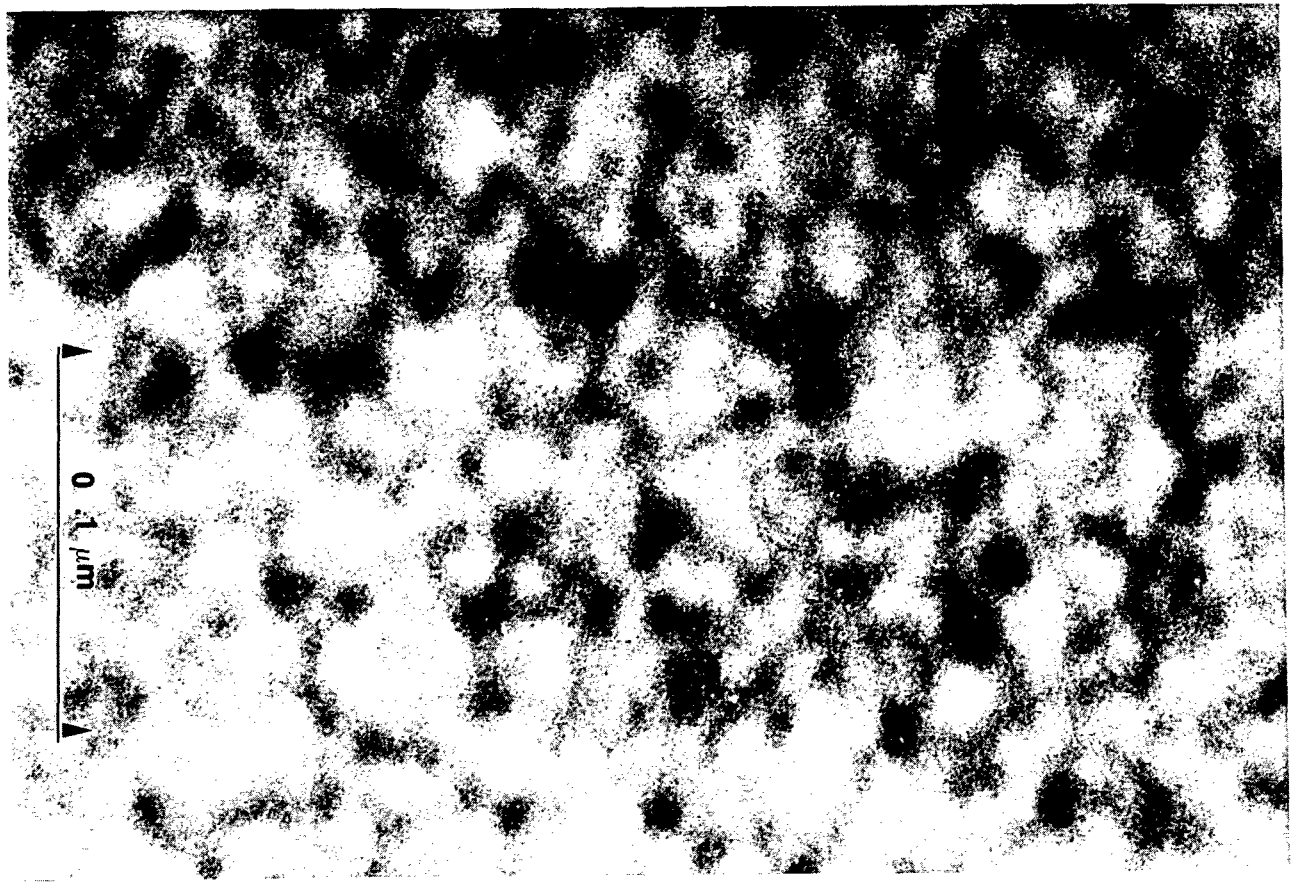

Fig. 13 Transmission micrograph of osmium tetroxide stained standard-cure sample containing 25 phr of mPDA.

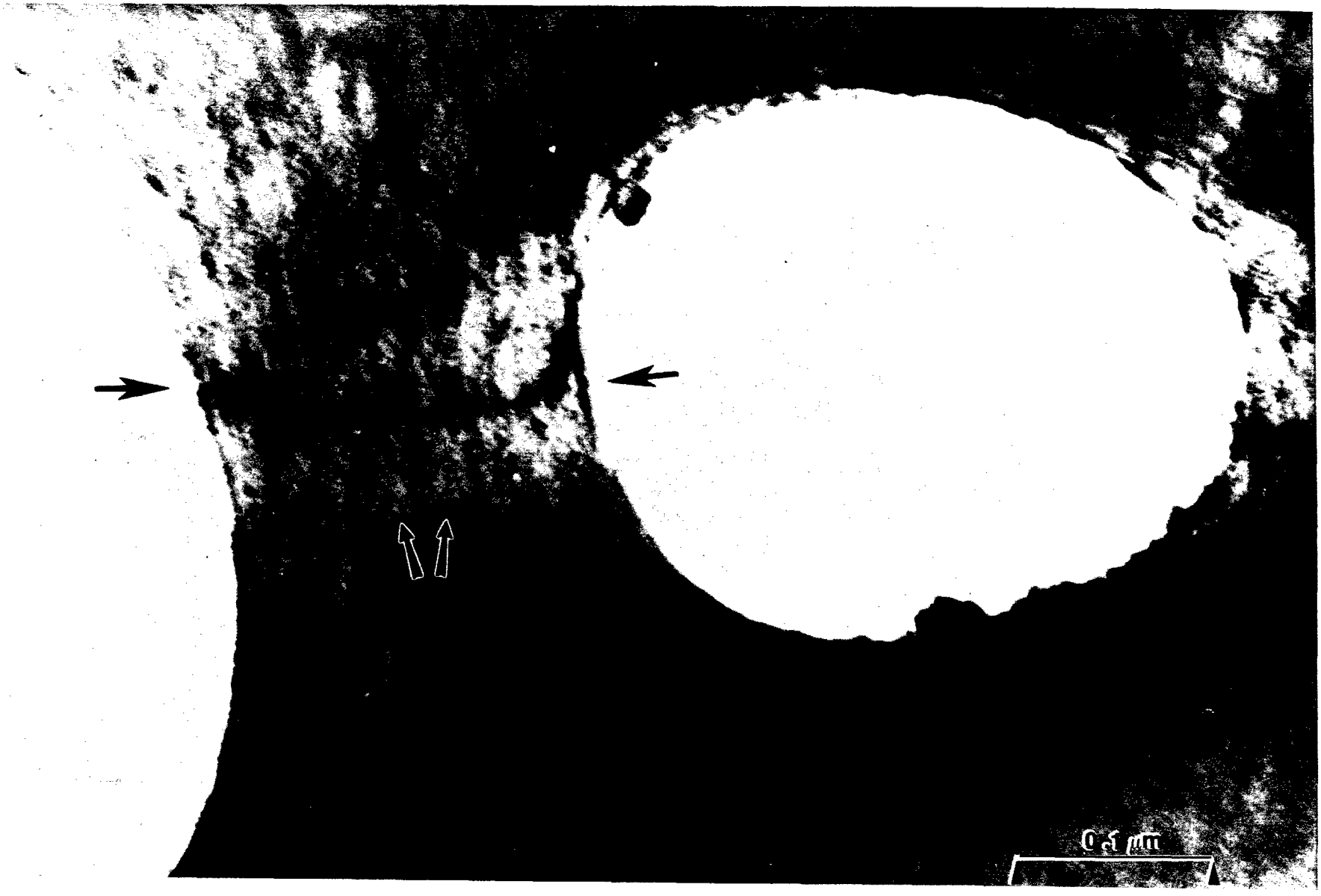

Fig. 14 Heterogeneities in a standard-cure stoichiometric sample around a propagating crack.

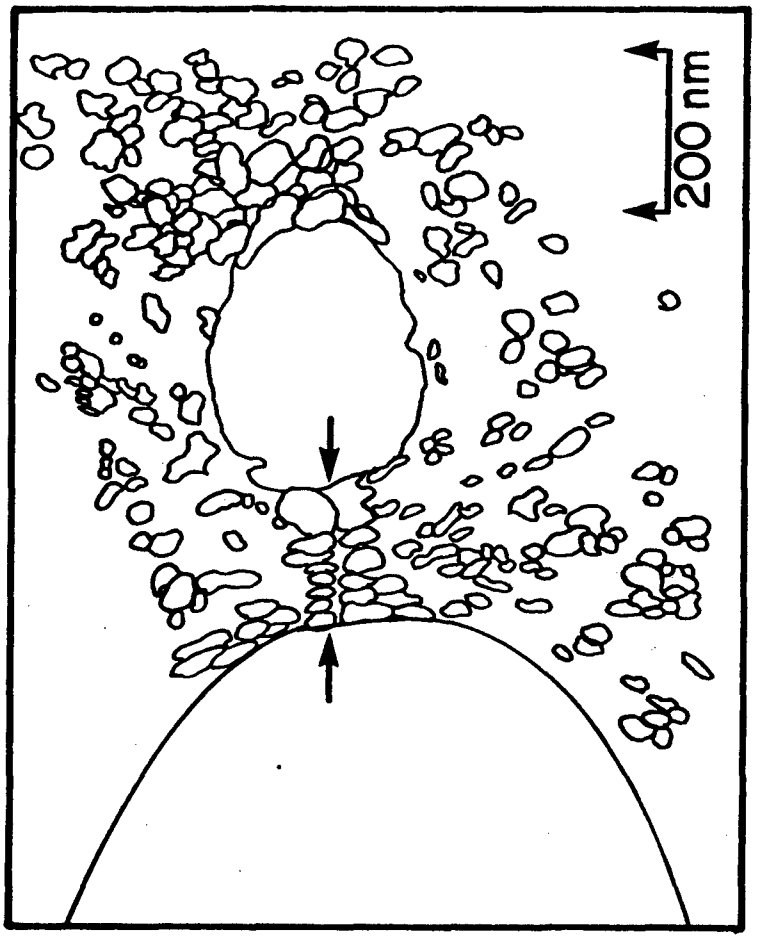

Fig. 15 The deformation and alignment of the heterogeneities around the propagating crack.

*U.S.Government Printing Office: 1987 —748-061/60688